Ultraviolet Electroluminescence from Randomly Assembled n-SnO_2 Nanowires$p$-GaN:Mg Heterojunction

H. Y. Yang,[†] S. F. Yu,[*,†] H. K. Liang,[†] S. P. Lau,[‡] S. S. Pramana,[§] C. Ferraris,[||] C. W. Cheng,[⊥] and H. J. Fan[⊥]

School of Electrical & Electronic Engineering, Nanyang Technological University, Singapore 639798, Singapore, Department of Applied Physics, The Hong Kong Polytechnic University, Hung Hum, Kowloon, Hong Kong, School of Materials Science and Engineering, Nanyang Technological University, Singapore 639798, Singapore, Laboratoire de Minéralogie et Cosmochimie, Muséum National d'Histoire Naturelle, CNRS 7202, CP52, 61 Rue Buffon, 75005 Paris, France, and Division of Physics and Applied Physics, School of Physical and Mathematical Sciences, Nanyang Technological University, Singapore 637371, Singapore

ARTICLE

ABSTRACT Electroluminescence characteristics of a heterojunction light-emitting diode, which was fabricated by depositing a layer of randomly assembled n-SnO_2 nanowires on p-GaN:Mg/sapphire substrate via vapor transport method, were investigated at room temperature. Peak wavelength emission at around 388 nm was observed for the diode under forward bias. This is mainly related to the radiative recombination of weakly bounded excitons at the shallow-trapped states of SnO_2 nanowires, Under reverse bias, near bandedge emission from the p-GaN:Mg/sapphire leads to the observation of emission peak at around 370 nm.

KEYWORDS: SnO_2 nanowires • light-emitting diodes • ultraviolet emission • defect state recombination

INTRODUCTION

SnO_2, which has bandgap (~3.6 eV) and exciton binding energies (~130 meV) larger than those of ZnO, is a semiconductor material suitable to realize short wavelength optoelectronic devices at and above room temperature (1). However, because of the dipole-forbidden nature (i.e., intrinsic bandedge transition is not allowed), SnO_2 may not be a promising ultraviolet (UV) luminescent material (2). Nevertheless, recent investigations have shown that the use of surface defect states to capture weakly bounded excitons can generate large UV excitonic gain in SnO_2 nanostructures via giant-oscillator-strength effect (3). In addition, the large surface area to volume ratio of SnO_2 nanostructrues significantly increases the amount of surface defects. As a result, intensive amplified spontaneous emission and random lasing action at UV wavelength were observed from SnO_2 nanostructures under high optical excitation (4).

Room-temperature electroluminescence (EL) at visible spectrum, which may be due to deep-trap states related to radiative recombination centers generated by defects or/and surface structures of SnO_2, was observed from n-SnO_2/p-Si and n-SnO_2/p-SiC heterojunctions (5, 6). However, the realization of SnO_2-based UV light-emitting diodes (LEDs) has not been reported. This is because the formation of surface defect states on SnO_2 nanostructures is sensitive on the fabrication parameters (i.e., including the proper use of substrate) (7). In this paper, we reported the growth of n-SnO_2 nanowires (NWs) on p-GaN:Mg/sapphire by vapor transport technique. It can be shown that the heterojunction formed between n-SnO_2 NWs and p-GaN:Mg/sapphire substrate can support UV emission at room temperature under forward bias. This is due to the radiative recombination of weakly bounded excitons occurs at the shallow-trapped states of n-SnO_2 NWs. Therefore, it is possible to realize SnO_2-based UV optoelectronic devices despite the dipole forbidden nature of SnO_2.

RESULTS AND DISCUSSION

Figure 1 shows the schematic of a heterostructural p-n junction diode. A 4×5 mm^2 p-GaN/sapphire substrate (from Technologies and Devices International, Inc.) was chosen to be the supporting substrate and hole-injection layer of the p-n heterojunction diode. About 700 nm thick randomly assembled n-SnO_2 NWs were deposited onto the surface of the p-GaN/sapphire substrate by vapor transport method (8) to form the heterojunction. Quartz substrate coated with indium tin oxide (ITO), which was in physical contact with the n-SnO_2 NWs, was used as a cathode of the heterojunction. This configuration was used to avoid direct deposition of ITO onto the SnO_2 NWs. Au (100 nm)/Ti (20 nm) metal layer was deposited onto the p-GaN layer as an anode ohmic contact.

Figures 2a shows the scanning electron microscopy (SEM) image of the SnO_2 NWs deposited on GaN. It is found that

* Corresponding author. E-mail: sfyu21@hotmail.com.
Received for review January 12, 2010 and accepted March 8, 2010
[†] School of Electrical & Electronic Engineering, Nanyang Technological University.
[‡] The Hong Kong Polytechnic University.
[§] School of Materials Science and Engineering, Nanyang Technological University.
[||] Muséum National d'Histoire Naturelle.
[⊥] School of Physical and Mathematical Sciences, Nanyang Technological University.
DOI: 10.1021/am1000294
2010 American Chemical Society

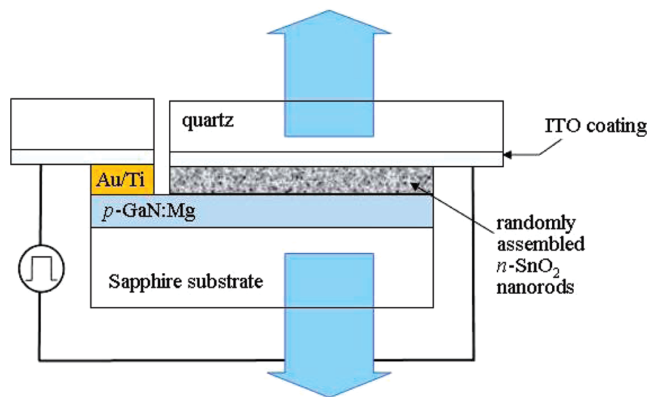

FIGURE 1. Schematics of a n-SnO_2 NWs/p-GaN:Mg/sapphire substrate heterojunction LED structure.

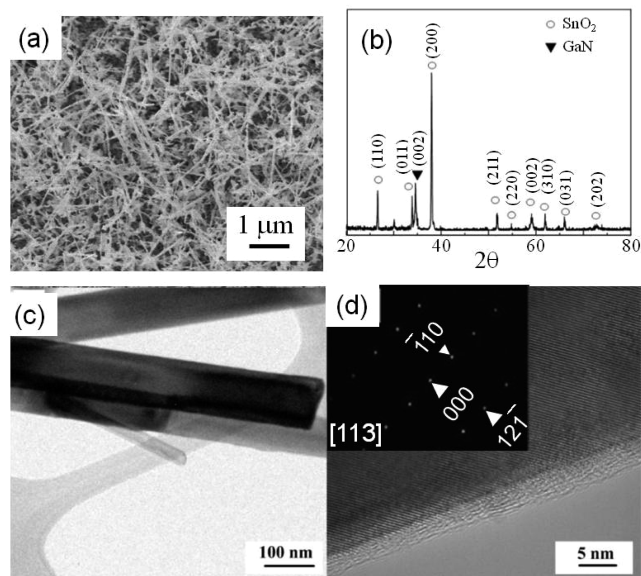

FIGURE 2. (a) SEM image and (b) XRD pattern of the randomly packed SnO_2 NWs grown on p-GaN substrate. (c) Bright0field and (d) high-resolution TEM image of a SnO_2 NW aligned along [113] direction. The inset shows an electron diffraction pattern of the SnO_2 NW.

the NWs have average length and thickness of $\sim$2 μm and $\sim$100 nm respectively, which are closely packed together to form a dense layer. Figure 2b gives the X-ray diffraction (XRD) pattern of the as-grown SnO_2 NWs. All the diffraction peaks can be indexed to the tetragonal rutile SnO_2 and no impurity phase was detected except the (002) GaN peak. Figure 2c shows the bright field transmission electron microscopy (TEM) image of a single SnO_2 NW. High-resolution TEM image and selective area electron diffraction (SAED) pattern, which were taken along [113] of the SnO_2 NW, are shown in Figure 2d. The high-resolution TEM image illustrates that the SnO_2 NWs have high-crystal-quality with lattice constants of $a = 4.73$ Å and $c = 3.17$ Å. It is also noted that the surface of the nanowires has an amorphous layer with an average thickness of 2.5 nm. This amorphous layer can be attributed to the formation of shallow trapped states for the occupation of excitons that lead to the generation of UV radiation. This is because the removal of amorphous layer by thermal oxidation has shown the suppression of UV radiation from the SnO_2 nanowires (3).

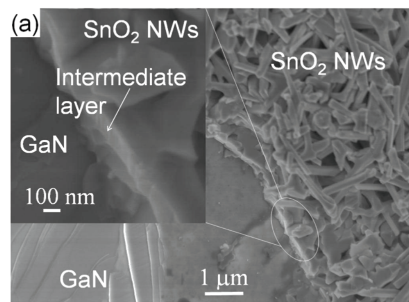

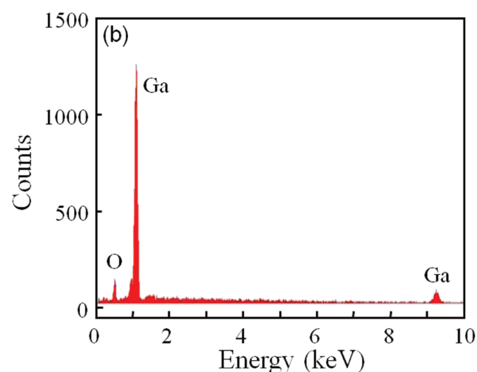

FIGURE 3. (a) Cross-sectional SEM image of the SnO_2 NWs-GaN interface. (b) EDS spectrum of the intermediate layer.

Figure 3a shows cross-sectional SEM images of the diode. An intermediate layer, which has a thickness of about 100 nm, is observed between the GaN substrate and SnO_2 NWs. It is believed that the intermediate layer is arisen from the oxidation of Ga from the GaN substrate's surface during the vapor transport process (9). Figure 3b plots energy-dispersive spectroscopy (EDS) spectrum of the intermediate layer. It is noted that elements Ga and O are the dominant peaks in the EDS spectrum and this indicated that intermediate layer is only composed of Ga and O. In addition, the molecular ratio between Ga and O in the intermediate layer calculated from the EDS data is close to that of Ga_2O_3.

Figure 4a shows the electroluminescence (EL) spectra of the heterojunction diode under forward bias that were measured from the surface of the SnO_2 NWs. A broad emission spectrum centered at $\sim$388 nm is recorded and the turn-on voltage of the diode is found to be +11.5 V. The insert displays a photo of the diode taken at forward bias of about +14 V. The blue-violet light emitted from the diode can be clearly seen from naked eyes even in normal office lighting environment. It is also noted that only the region of SnO_2 NWs covered with the ITO/quartz substrate has intensive UV radiation. Hence, the observed UV radiation is mainly due to the recombination of electrons injected into the SnO_2 NWs layer with holes provided by the p-GaN layer. In addition, excitonic recombination is the main radiative recombination process taking place inside the SnO_2 NWs. It is believed that the radiative recombination of weakly bounded excitons at the shallow-trapped states, which arise from the surface defects states presented in the amorphous layer of the SnO_2 NWs, contributes to the UV emission (3, 4).

Emission characteristics of the heterojunction diode under reverse bias were also investigated. This is because

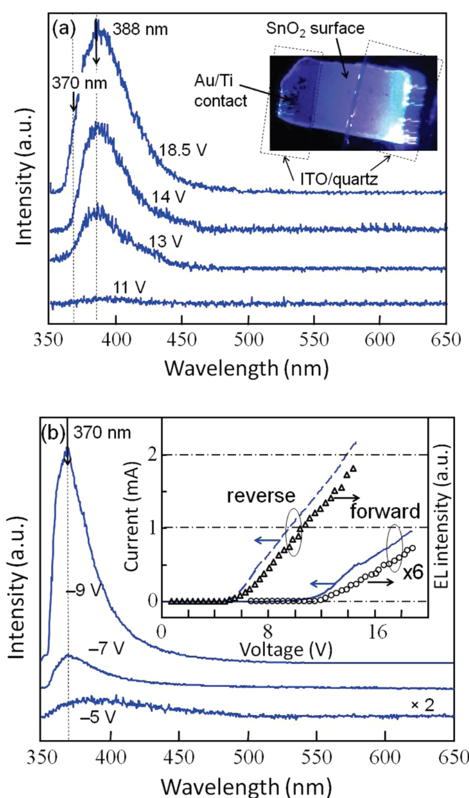

FIGURE 4. (a) Room-temperature EL spectra of the heterojunction LED at various forward bias voltages. The insert shows the color photo taken for the LED under a forward bias voltage of 14 V. (b) EL spectra under various reverse bias from top surface of the LED at room temperature. The insert shows the room-temperature $I-V$ characteristics of the n-SnO_2 NWs/p-GaN:Mg/sapphire substrate heterojunction LED under forward and reverse bias voltage.

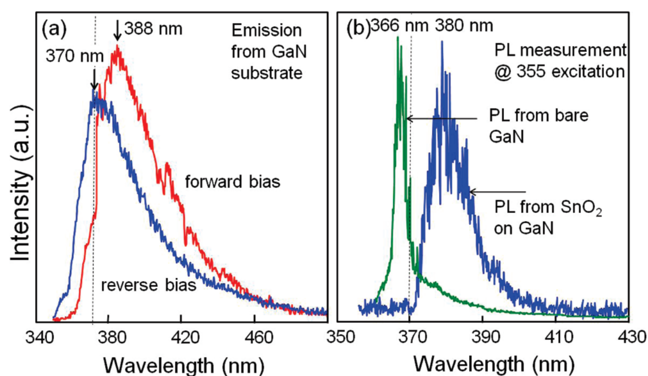

FIGURE 5. (a) EL spectrum of the heterojunction measured from the p-GaN:Mg/sapphire substrates under forward bias and reverse bias. (b) Normalized room temperature PL spectra of the n-SnO_2 NWs and p-GaN:Mg/sapphire under optical excitation by a frequency-tripled Nd:YAG laser (355 nm) at pulsed operation (6 ns, 10 Hz).

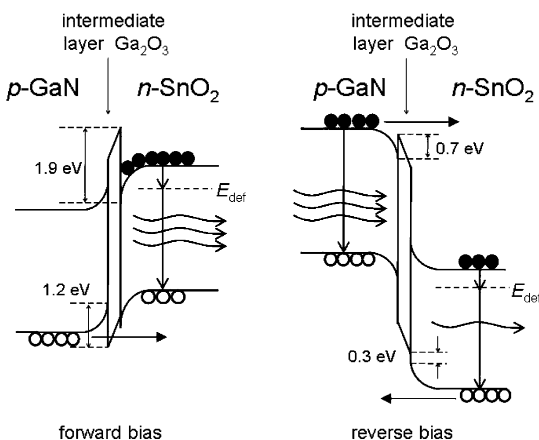

FIGURE 6. Schematic diagram showing the energy band alignment of the n-SnO_2/Ga_2O_3/p-GaN heterojunction under forward and reverse bias.

carrier transport involving tunneling through the nanostructured heterojunction is also possible to realize UV radiative recombination (10). Figure 4b plots the EL spectra of the heterojunction diode under reverse bias. An intense emission spectra with peak wavelength at ~370 nm is observed, which is due to the near bandedge emission of GaN. As the observed emission peak wavelength is different to that under forward bias, it is believed that holes from the unoccupied conduction band minimum of n-SnO_2 NW are also injected into the occupied valence band maximum of p-GaN under reverse bias. The inset of Figure 4b compares the current–voltage and intensity–voltage curves of the n-SnO_2 NWs/p-GaN heterojunction diode under forward and reverse bias. It is noted that the UV emission intensity observed from the diode under reverse bias is much higher than that under forward bias. This indicated that the diode is more effective to achieve carrier transport through the heterojunction during reverse bias so that the magnitude of turn-on voltage at reverse bias is lower than that of forward bias.

The characteristics of EL spectra collected from the surface of the sapphire substrate (i.e., collected from the supporting substrate) were also investigated. Figure 5a shows the emission spectra for the heterojunction diode under a forward bias at +14 V and a reverse bias at −7 V. It is observed that the emission peak under forward (reverse) bias is ~388 nm (~370 nm), which matches the value obtained from the surface of SnO_2 NW layer. As the EL spectra observed from both sides of the diode have similar peak emission wavelength, the intermediate layer should has a bandgap wider than that of the GaN substrate and SnO_2 NWs.

Figure 5b shows the room-temperature photoluminescence (PL) spectra measured from the randomly assembled SnO_2 NWs grown on a p-GaN substrate as well as from a bare p-GaN:Mg/sapphire substrate. The PL peak emission wavelength and bandwidth observed from the surface of the SnO_2 NWs (bare p-GaN substrate) are found to be ~380 (~366) nm and ~17 (~6) nm respectively under optical excitation at ~0.4 MW/cm^2. By comparing the peak wavelength and bandwidth of the PL spectra with that of the EL spectra, it is believed that radiative recombination inside the n-SnO_2 NWs (p-GaN substrate) is dominant for the diode under forward (reverse) bias. However, the difference in peak wavelength and bandwidth of emission spectra indicates that the energetic injection carriers under electrical pumping have changed the radiative recombination process on both sides of the heterojunction.

The radiative recombination process of the heterojunction diode can be understood in terms of the energy-band diagram, as shown in Figure 6. It is assumed that the vacuum levels of the n-SnO_2 NWs, p-GaN:Mg substrate, and interme-

ARTICLE

diate layer are continuously across the heterojunction by perfect contacting. Electron affinity energies of n-SnO_2 and p-GaN are assumed to be 4.53 and 3.3 eV, respectively (5, 11). In addition, the bandgap energy of SnO_2, is taken to be about 3.6 eV and that of p-GaN:Mg is assumed to be 3.3 eV (5, 11). It is also assumed that the intermediate layer is made of Ga_2O_3 with bandgap energy and electron affinity approximately equal to 5.2 and 2.5 eV respectively (12, 13). Hence, it can be shown that the conduction band offset (ΔE_C) and valence band offset (E_V) of the p-GaN/Ga_2O_3 (Ga_2O_3/n-SnO_2) interface are roughly equal to 0.7 (1.9) and 1.2 eV (0.3 eV) respectively. For the heterojuniction under forward bias, the injection of electron from n-SnO_2 to p-GaN is blocked by the intermediate layer (i.e., ΔE_C is 1.9 eV) so that the tunneling of hole through the intermediate layer determines the overall current of the heterojunction. As a result, radiative recombination (between the defect energy level, E_{def}, and the valence band of SnO_2 NWs) is dominant inside the SnO_2 NWs (14). This may also be the reason why the turn-on voltage is large for the forward bias case. For the heterojunction under reverse bias, electrons injected from p-GaN to n-SnO_2 are slightly blocked by the intermediate layer because of the small value of ΔE_C (~0.7 eV) of the p-GaN/Ga_2O_3 interface. In addition, holes experience no barrier between n-SnO_2 and p-GaN. As a result, radiative recombination is supported on both sides of the heterojunction but the emission is dominant inside p-GaN:Mg substrate (15). These also explained the reasons why the turn-on voltage (EL intensity) for the reverse bias case is smaller (larger) than that for the forward bias case. On the other hand, if the Ga_2O_3 intermediate layer is not presented, radiative recombination will be supported inside both p-GaN and n-SnO_2 layers simultaneously under either forward or reverse bias. This is because the electrons and holes have the same transportation probability across the heterojunction.

SUMMARY

In summary, UV EL has been demonstrated from n-SnO_2 NWs/p-GaN heterojunction LED operating at room temperature. Under forward bias, peak emission wavelength at around 388 nm, which is mainly related to the radiative recombination of weakly bounded excitons at the shallow-trapped states of SnO_2 nanowires, was observed. Under reverse bias, emission peak at around 370 nm was observed due to near bandedge emission from the p-GaN:Mg/sapphire. This is because of the presence of an intermediate Ga_2O_3 layer, which suppressed the injection of electrons to the p-GaN:Mg under forward bias, formed between n-SnO_2 NWs and p-GaN:Mg/sapphire substrate. As a result, UV emission observed under forward bias is dominant by the radiative recombination of weakly bounded excitons inside the SnO_2 NWs. Hence, it is verified that the possibility to realize SnO_2-based UV optoelectronic devices despite the dipole forbidden nature of SnO_2.

FABRICATION AND MEASUREMENT METHODS

Fabrication. The heterojunction diode was fabricated by vapor transport technique. A p-GaN substrate coated with ~3 nm thick of Au and an alumina boat with source powder (a mixture of SnO_2 and graphite with weight ratio 1:1) were placed inside a small quartz tube (diameter 15 mm, length 300 mm). The substrate was placed 7 cm away from the center of the boat. The quartz tube was then positioned inside a horizontal furnace in which the temperature and pressure were maintained at 1050 °C and ~20 mbar respectively. In addition, Ar mixed with 5% of O_2 was used as a carry gas. After 30 minutes of deposition, a ~600 nm thick of light-gray film, which has an electrical conductivity of 0.4 Ω cm, was formed on the p-GaN substrate. The morphology and crystalline of the nanostructures were characterized by a SEM (JSM 6340F) and a TEM (JEM 2010). Bilayer Ti (20 nm)/Au(100 nm) electrode was deposited on the p-GaN:Mg as the ohmic contact.

EL and PL Measurement. The heterojunction diode was driven by a rectangle pulse voltage source with repetition rate and pulse width of 7.5 Hz and 80 ms, respectively. Light was collected from either the uncoated side of the quartz substrate or the sapphire substrate by an objective lens. PL spectra of the samples at room temperature were studied under optical excitation by a Nd:YAG (355 nm: YAG: yttrium aluminum garnet) laser operating in pulsed mode (6 ns, 10 Hz). Optical pumping was achieved by using a cylindrical lens to focus a pump stripe of length ~ 5 mm and width ~50 μm on the surface of the samples. Emission was also collected in the direction perpendicular to the surfaces of the samples.

Acknowledgment. This work was supported by LKY PDF 2/08 startup grant.

Note Added after ASAP Publication. In the version of this paper published to the Web on March 15, 2010, the author C. Ferraris was incorrectly listed as F. Cristiano. The corrected version was published to the Web on March 30, 2010.

REFERENCES AND NOTES

(1) Yu, B. L.; Zhu, C. S.; Gan, F. X. *Opt. Mater.* **1997**, *7*, 15–20.
(2) Agekyan, V. T. *Phys. Status Solidi, A* **1977**, *43*, 11–42.
(3) Liu, R. B.; Chen, Y. J.; Wang, F. F.; Cao, L.; Pan, A. L.; Yang, G. Z.; Wang, T. H.; Zou, B. S. *Physica E* **2007**, *39*, 220–229.
(4) Yang, H. Y.; Yu, S. F.; Lau, S. P.; Tsang, S. H.; Xing, G. H.; Wu, T. *Appl. Phys. Lett.* **2009**, *94*, 241121.
(5) Yuan, Z. Z.; Li, D. S.; Wang, M. H.; Chen, P. L.; Gong, D. R.; Cheng, P. H.; Yang, D. R. *Appl. Phys. Lett.* **2008**, *92*, 121908.
(6) Yang, H. Y.; Yu, S. F.; Cheng, C. W.; Tsang, S. H.; Liang, H. K.; Fan, H. J. *Appl. Phys. Lett.* **2009**, *95*, 201104.
(7) Mazeina, L.; Picard, Y. N.; Caldwell, J. D.; Glaser, E. R.; Prokes, S. M. *J. Cryst. Growth* **2009**, *311*, 3158–3162.
(8) Dai, Z. R.; Pan, Z. W.; Wang, Z. L. *Adv. Function. Mater.* **2003**, *13*, 9.
(9) Dong, Y.; Feenstra, R. M.; Northrup, J. E. *Appl. Phys. Lett.* **2006**, *89*, 171920.
(10) Park, W. I.; Yi, G. C. *Adv. Mater.* **2004**, *16* (1), 87–90.
(11) Grabowski, S. P.; Schneider, M.; Nienhaus, H.; Monch, W.; Dimitrov, R.; Ambacher, O.; Stutzmann, M. *Appl. Phys. Lett.* **2001**, *78*, 2503–2505.
(12) Ji, Z. G.; Du, J.; Fan, J.; Wang, W. *Opt. Mater.* **2006**, *28*, 415–417.
(13) Gowtham, S.; Deshpande, M.; Costales, A.; Pandey, R. *J. Phys. Chem. B* **2005**, *109*, 14836–14844.
(14) Sze, S. M. *Physics of Semiconductor Devices*, 2nd ed.; John Wiley & Sons: New York, 1981; Chapter 7.
(15) Wu, M. K.; Shih, Y. T.; Li, W. C.; Chen, H. C.; Chen, M. J.; Kuan, H.; Yang, J. R.; Shiojiri, M. *Photon. Technol. Lett.* **2008**, *20* (21), 1772–1774.

AM1000294